FEATURES OF THE MORPHOLOGY OF THE SHEAR FAILURE SURFACES OF COARSE-GRAINED SLIP ZONE SOILS

Zechuang Li [1], Qiyuan Cai[1] and Di Liu[2]

1. *School of Civil Engineering, Northeast Forestry University, Harbin 150040, Heilongjiang, China;lzc@nefu.edu.cn, caiqiyuannefu@163.com*
2. *Zhejiang Huadong Construction Engineering CO., LTD, Hangzhou 310014, Zhejiang, China; liu_d5@hdec.com*

ABSTRACT

Analyzing the change in the roughness of the shear failure surface under different particle composition is important to reveal the mesoscopic mechanism of strength change of coarse-grained slip zone soil. Slip zone soils were grouped according to different particle gradations and coarse particle contents for experiments. To collect shear surface coordinate data points, the customized shear surface measurement mold was examined to measure the shear surface. Then, the measured 3D elevation data are drawn into a 3D surface map by using the Surfer software to show the actual situation of the shear surface. The shear surfaces were analyzed by using box plots and ice crystal flower plots. Finally, the roughness of the shear surface was quantified by the root mean square of the relative undulation (Z_2). Findings indicate that the shear surface undulation characteristics of coarse-grained slip zone soil are obviously correlated with the proportion of particles with a size between 5–20 mm. Moreover, whether the gradation is good or poor has a significant effect on the shear surface characteristics. The well-graded shear surface is rougher and more undulated, whereas the poorly graded shear surface is the opposite. As the normal pressure increases, the roughness of the shear surface decrease. As the content of coarse particles increases, the roughness of the shear surface increases, and Z_2 has a highly positive linear correlation with the coarse particle content.

KEYWORDS

Slip zone soil, Shear surface, Roughness, Medium direct shear test, Meso-structure

INTRODUCTION

The shear strength of slip zone soils is one of the most important factors in landslide stability evaluation and landslide protection and management. Few studies have been conducted on shear surface characteristics, and most of them focus on structural plane of rock and soil aggregate and rock [1-2]. Currently, research on the shear surface characteristics of slip zone soil is still lacking.

Scholars who studied the shear properties of weathered schist residual soils found that the undulation of shear surface increases with increasing stone content. With the increase in the normal pressure, mostly tumbling and gnawing failure occur [3]. Some scholars also found through large-scale shear experiments of coarse grain soil that the shear surface has an obvious undulating shape

[4]. An experimental study of the shear character of rock and soil aggregate found that the shear surface has a good fractal property and calculated the fractal dimension of the shear surface [5]. In their study on gravelly slip zone soils, Ren et al. [6] found that the residual strength is determined by the contact properties of gravels on the shear surface and the shear surface undulation. Many studies have found that the morphological features of the shear surface have an effect on the strength, but no studies have been conducted on the effect of factors such as particle gradation and coarse particle content on the shear surface nor have they been able to establish a good relationship between shear surface undulation and shear strength. At present, no dedicated instrument for measuring the shear surface is available; the most common solution in this research field is to obtain the data point cloud of the shear surface by 3D laser scanning technology [7-8]. However, 3D laser scanning is an expensive technique for collecting point clouds of 3D data.

In this paper, the shear surface of slip zone soil is first measured by using the hanging wire method by studying the customized mold. The samples can be measured immediately after shearing, and the measurement accuracy can meet the requirements of analysis. Then, the Surfer software is used to draw the measured data into a 3D surface map to reflect the features of the shear surface more clearly. Analyze the 3D surface map, build meso-structural models to observe internal structures, and conduct further statistical analysis of shear surfaces through box plots and ice crystal flower plots. Finally, the roughness of the shear surface is quantitatively described by the root mean square of relative undulation, and the features of the shear surface of the slip zone soil with different particle compositions are analyzed.
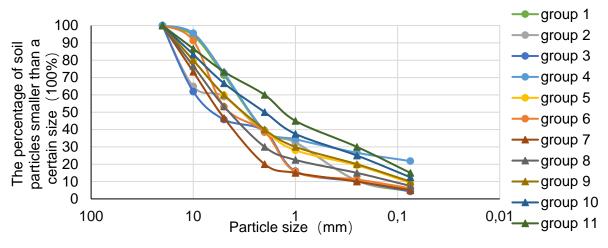
TEST MATERIALS AND METHODS

Soil samples were taken from the landslide on the south slope of the West Open-pit Mine in Fushun [9]. Reconstituted test specimens consisted of dried and sieved soil samples of each particle size. The sieving particle size range is 0–0.075, 0.075–0.25, 0.25–0.5, 0.5–2, 2–5, 5-10, and 10–20 mm. The test does not consider particle breakage, and the coarse particles that are larger than 2 mm are replaced with white stones, as shown in Figure 3(a). The test uses a medium-sized direct shearing instrument. The direct shear box internal length and width are 200 mm, and the height of the upper and lower shear boxes is 100 mm.

(1) Shear test scheme: To investigate the effect of different particle compositions on the shear failure surface undulation of slip zone soil, coarse-grained slip zone soil was divided into seven groups according to different particle size distributions. The first, second, and third groups were poorly graded, and the fourth, fifth and sixth groups were well graded (particles with a size greater than 2 mm are considered coarse grains [10]). The soil was then divided into five groups according to the content of coarse particles, and groups 7, 8, 9, 10, and 11 have coarse particle contents of 40%, 50%, 60%, 70%, and 80%, respectively. In the group with coarse particle content, the gradation of coarse particles above 2 mm and the gradation of fine particles below 2 mm were equally divided. Here, 40% coarse particle content was taken as an example; 0–0.075, 0.075–0.25, 0.25–0.5, 0.5–2, 2–5, 5–10, and 10–20 mm accounted for 15.00%, 15.00%, 15.00%, 15.00%, 13.33%, 13.33%, and 13.33%, respectively. Each group was tested under three different normal pressures of 50, 100, and 150 kPa. The "Standard for Geotechnical Test Methods GB/T50123-2019" serves as a reference for the test shear process [11]. The topographic geometry of the sheared surface was measured
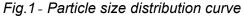
after shearing. The particle size distribution curve is shown in Figure 1.

Fig.1 – Particle size distribution curve

(2) Shear surface 3D elevation data point acquisition: A measuring mold was made to extract the 3D data points of the shear surface. To make the mold fit well with the shear box, the length and width of the mold are designed to be consistent with the upper and lower shear boxes. The leg height is 60 mm. The mold schematic is shown in Figure 2(a), and the actual mold is shown in Figure 2(b). Two crawlers of the same width as the mold frame are fixed above the mold sides, The mold is equipped with a steel rod with indentations, as shown in Figure 2(c), and a hanging hammer with scale, as shown in Figure 2(d). The four legs of the mold are placed on the shear box, the steel rods are placed in the corresponding grooves on both sides of the crawlers in turn. And the hanging wire method is used for measurement, that is, the specific measurement method in the subsequent paragraph. The plane size of the soil sample is 200 mm × 200 mm. To exclude edge effects, only the 104 mm × 104 mm area in the center of the shear surface was measured (Figure 3a). The groove spacing of the mold crawler is 8 mm, that is, the Y-coordinate point spacing. The indentation spacing of the steel rod is 8 mm, that is, the X-coordinate point spacing. Thus, the coordinates of horizontal X and Y are determined (X is the shear direction). The hanging wire method is as (3).
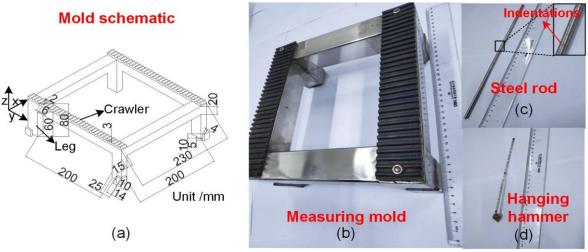

Fig.2- Drawing of the shear surface measurement mold: (a) schematic of mold; (b) actual mold; (c) actual steel rod; (d) actual hanging hammer

(3) The hanging hammer was dropped perpendicularly along the indentations of the steel rod, and the process was stopped when the hammer just touched the shear surface (i.e., shear failure surface). According to the scale of the thin line, the height of the drop of the hanging hammer from the upper surface of the steel rod is read and then marked as h_1. The vertical distance from the upper surface of the steel rod to the upper surface of the lower shear box is h_0. $Z = h_1 - h_0$ is the elevation of the measured point, that is, the coordinate Z represents the elevation of this point on the shear surface. The actual measurement process is shown in Figure 3(b).
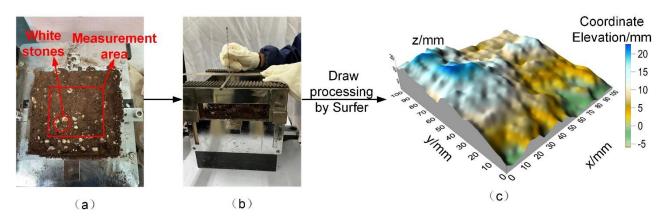

Fig.3- Extraction process of the 3D topography of the shear surface: (a) the actual shear surface after shearing; (b) the measurement diagram of the shear surface; (c) the 3D topography map of the shear surface

ESTABLISHMENT OF THE MESO-STRUCTURAL MODEL

The random filling algorithm is used to establish the meso-structure model by using MATLAB programming language. The established space size is consistent with the test shear box size, which is 200 mm × 200 mm, and the area is denoted as "*A*." According to the particle size gradation in the test scheme, the diameter range of each particle interval and the proportion of particles in each particle interval is set, and the proportion coefficient is recorded as "*p*." The principle is as follows: First, the sequence randomly picks a point "*O*" in the space, with the point as the center of the ellipse [12]. An ellipse with the length of the long semi-axis "*a*" and the length of the short semi-axis "*b*" is generated. "*a*" is the radius of the largest particle in the particle interval. After the ellipse is generated, a part of the arc is randomly picked to translate and deform inward at equal distances; it is regarded as a new particle after deformation. Then, a point in space is picked again. If the point is within the range of generated particles, then a new point is picked, and if it is outside the range of generated particles, then the minimum distance between the point and the outer surface of particles is calculated. If the distance is less than the maximum radius of the particle size interval, then a new point is picked, and if the distance is greater than the maximum radius of the particle size interval, then a particle is generated according to the above steps. The distance from any point in the plane to the boundary of the particle is shown in the literature [12-13].

The criterion of the position relation between points and particles on the plane is as follows:

Consider the function: $\varphi(x,y) = (x-x_0, y-y_0)A\begin{pmatrix} \dfrac{1}{a^2} & 0 \\ 0 & \dfrac{1}{b^2} \end{pmatrix} A'\begin{pmatrix} x-x_0 \\ y-y_0 \end{pmatrix} - 1$ (1)

Let $P(x,y)$ be a point on the plane. If $\varphi(x,y) > 0$, then $P(x,y)$ is outside the particle. If

$\varphi(x,y) = 0$, then $P(x,y)$ is on the particle. If $\varphi(x,y) < 0$, then $P(x,y)$ is inside the particle.

The principle of particle deformation is as follows:

The interval of symmetry for "a_0" [13]: $[a_0 - r_1, a_0 + r_1]$ and $[a_0 - r_2, a_0 + r_2]$, among them $0 \leq r_1 < r_2$,

let $t = (x-a_0)^2$. The C function is then created $g(x,a_0,r_1,r_2) = g(t) = \begin{cases} e^{\frac{1}{(t-r_1^2)(t-r_2^2)}}, & 0 \leq r_1^2 < t \leq r_2^2 \\ 0, t \leq r_1^2, t \geq r_2^2 \end{cases}$ (2)

Scaling factor: $B(x,a_0,r_1,r_2) = \begin{cases} 1, & t \leq r_1^2 \\ \int_{0.025 r_1^2}^{r_2^2} g(s)ds \Big/ (\int_{4r_1^2}^{r_2^2} g(s)ds + 0.01), & r_1^2 < t \leq r_2^2 \\ 0, & t > r_2^2 \end{cases}$ (3)

This factor is used to randomly translate inward at equal intervals to achieve a deformation effect.
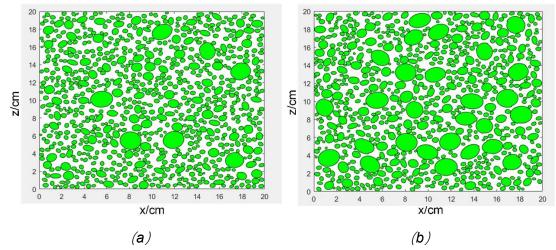

(a)   *(b)*

Fig.4- Meso-structure model diagram: (a) first group of gradation; (b) gradation for group 9

In this way, the particles are generated cyclically, and the total area of the generated particles is calculated. The ratio of the sum of the areas of all particle sizes to the space area *A* is *q*, and the ratio of this particle size range to all particle sizes is p_1. When the area of generated particles exceeds $q \times p_1 \times A$, the generation of the particle size is stopped. The next particle size is generated until all particle sizes have been generated. The generation of small particle sizes is too complicated; thus, only the particle size larger than 2 mm is simulated. The generated model is shown in Figure 4.

ANALYSIS OF TEST RESULT

Effects of particle gradation on shear surface undulation morphology

To more specifically reflect the morphology of the shear failure surface, the measured 3D data points were drawn with Surfer. The following is a comparative analysis:

Comparison between 3D topography map and actual shear surface

First, the actual shear surface is compared with the figure drawn by Surfer to show the actual situation corresponding to the 3D topography map more clearly.
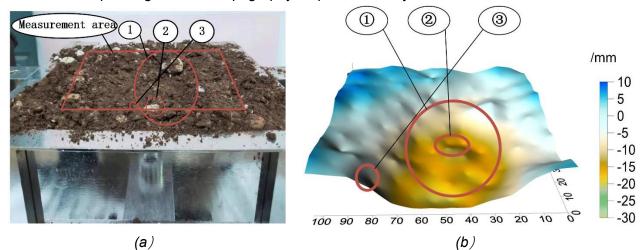

(a)　　　　　　　　　　　　　　　　*(b)*

Fig.5- Comparison between the shear surface 3D topography map and the actual shear surface: (a) the actual shear surface; (b) the shear surface 3D topographic map

①, ②, and ③ in Figure 5(a) correspond to ①, ②, and ③ in Figure 5(b). The ① in the two sub-figures is due to the fact that this part is relatively compact, with good particle interlocking, good internal structure integrity. In the shearing process, this part could not be cut off because of its strong shear resistance and appeared as a large regional depression. The ② is due to the protrusions being supported by coarse particles, and it has high strength. During shearing, the protrusions could not be cut off but passed over. After the upper shear box is removed, this part appears as a small protrusion. The ③ is due to the poor interlocking between a single coarse particle and the soil in the lower shear box, which is more firmly embedded with the upper shear box. During shearing, this particle pushes the particles around the inlay part of the lower shear box loose and move backward, forming small pits.

Comparative analysis of well-graded soil and poorly graded soil

Figure 6 compares well-graded and poorly graded groups: Three groups (2, 5 and 6) with similar contents of 5-20mm were selected for comparative analysis.

Comparison at 50 kPa: The figure shows many small protrusions and pits in all three figures. However, compared with the poorly graded group 2 (Figure 6c), the well-graded groups 6 (Figure 6a) and 5 (Figure 6b) have obviously protrusions and depressions. (i.e., obvious undulation)

Comparison at 100 kPa: Compared with the poorly graded group (Figure 6f), the well-graded

group in group 6 (Figure 6d) has more obvious undulation and is rougher. Group 5 (corresponding to Figure 6e) with good gradation has similar overall undulation to group 2 with poor gradation.
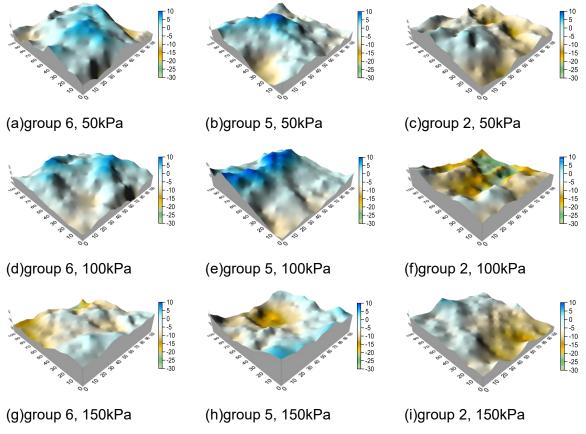

(a)group 6, 50kPa	(b)group 5, 50kPa	(c)group 2, 50kPa
(d)group 6, 100kPa	(e)group 5, 100kPa	(f)group 2, 100kPa
(g)group 6, 150kPa	(h)group 5, 150kPa	(i)group 2, 150kPa

Fig. 6- Comparison of shear surface topography (well- and poorly graded soil, Unit: mm)

Comparison at 150 kPa: Groups 6 (Figure 6g) and 5 (Figure 6h) are two well-graded test groups with different shear surface undulations, but both are more obvious than the poorly graded group 2 (Figure 6i). In addition, Figures 6(e), 6(g), and 6(i) all exhibit shear inclination. Thus, the gradation of coarse-grained soil has an obvious influence on the roughness of shear surface. The shear surface of the well-graded group has an obvious interlocking bond and is rougher than that of the poorly graded group. Most of the protrusions of the poorly graded groups were cut off and the shear surface was relatively smooth because the protrusions with an inclination angle >0° can act as resistance during shearing. The poorly graded group does not have a good interlocking bond, the protrusions are more likely to be sheared off, and the resistance to shear in the shearing process is relatively small. In contrast, the well-graded group has good particle interlocking, the protrusions are not easily sheared off, and the resistance to shear in the shearing process is relatively large. All the above-mentioned particle gradations were grouped separately at different normal pressures. The comparison derived that the shear surface is the smoothest under 150 kPa, the second under 100 kPa, and the roughest under 50 kPa. The comparative analysis of different normal pressure concluded that, with the increase in the normal pressure, the roughness of shear surface decreases and becomes smoother. During the shearing process, the occurrence of shear displacement needs to overcome the occlusion between the protrusions and the sliding friction resistance of the shearing surface. When the normal pressure is not enough, the upper soil sample climbs along the protrusions

of the shear surface so as to balance the vertical force caused by shear (it is characterized by shear expansion). When the normal pressure is large enough, the climbing movement is inhibited and the shear strength increases. When the shear force increases to a certain extent, the protrusion is sheared off. The shear failure of the protrusions is determined by its shear resistance.

Statistical analysis of coordinate elevation of shear failure surface

The elevation (Z) of 3D data points on the shear failure surface measured after shearing was statistically analyzed, and the box graph was drawn as follows. In Figure 7, "group 1, 50 kPa" represents the group 1 sample sheared under normal pressure of 50 kPa.
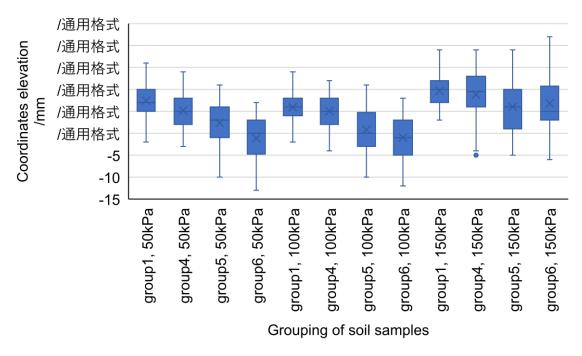

Fig.7- Elevation statistics of shear failure surface coordinates

To study the influence of particle proportion between 5–20 mm on the shear failure surface undulation morphology, the particle content in the interval was taken as a variable, and the test results under normal pressure of 50, 100, and 150 kPa were analyzed, taking one group of poor gradation and three groups of good gradation as examples (the proportion of 5–20 mm particles in groups 1, 4, 5, and 6 was 28.67%, 27.39%, 40.21%, and 46.79%, respectively). A large difference between the upper and lower edges of the box plot and difference between the upper and lower quartiles corresponds to a sparse elevation of the shear surface, that is, the probability of a rougher shear surface is greater. The figure clearly shows that under the normal pressure of 50 and 100 kPa, the box plot of the 3D coordinate points of the shear surface shows a downward trend as a whole with the increase in the proportion of particles between 5–20 mm. This finding does not mean that the roughness decreases, but that the elevation of the shear surface generally decrease with the increase of particles in the interval (i.e., 5-20mm). In addition, the difference between the upper and lower edges and the difference between the upper and lower quartiles gradually increase with the increase in the proportion of particles in the interval. This finding indicates that the shear surface becomes relatively rough and the undulation is larger with the increase in the proportion of particles

with a size between 5–20 mm. The overall decrease trend of the shear surface elevation with the increase in the particle size occurs because when the coarse particles are relatively few, a large part of the fine particles in the soil sample do not have enough coarse particles to combine and more fine particles combine; the combination of coarse and fine particles is stronger than that of fine particles. In the shear process, a regional zone is formed in the soil by the combination of many fine particles, and the protrusions supported by coarse particles near the shear zone have higher strength. Thus, the soil sample is cut apart along the regional zone where many fine particles are bound. Under the normal pressure of 150 kPa, although no sufficiently obvious rule is observed similar to that under the normal pressures of 50 and 100 kPa, the above changes still have a tendency to occur.
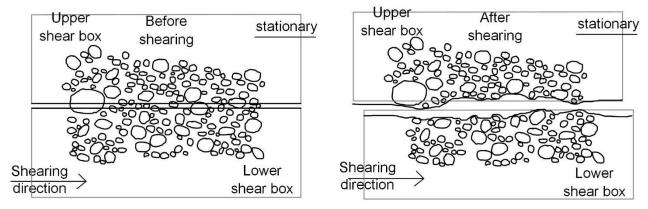

Fig.8- Schematic of the development of shear surface (the first group of grading)

In the first group of meso-structure, coarse particles are significantly fewer, and the distance between them is relatively large, so that they cannot form a good solid matrix. The pores between the coarse particles are filled with fine particles to form a solid matrix suspension structure. During the shearing process, most of the protrusions are easily sheared off, so the shear surface appears relatively flat.

Statistical analysis of undulation angle of shear surface profile along shear direction

A row of data points on the shear failure surface along the shear direction was statistically analyzed, and the angles between two adjacent points in a row of data were calculated, which were drawn in a polar coordinate system as an ice crystal flower diagram in the Figure 9. The proportion of particles between 5–20 mm is still used as the variable for comparison, and the normal pressure is 50 kPa as an example. Statistical analysis of all data points showed that an angle greater than 45° is very rare. Therefore, for the convenience of processing, the angle over 45° is calculated as 45°. In the figure, there is a column of shear surface data every 45°. Fourteen columns of shear surface data exist for each group of specimens, and 8 columns of the middle part are selected to draw a complete 360° graph. The first region in order is the most marginal column of data, arranged inward in order, and the fourth and fifth regions are the innermost two columns of data in the shear surface. In the actual shear surface, part of area 1 is relatively flat, and another part is undulating. The ice crystal flower diagram shows that part of the angle of area 1 is close to 0°, and most angles are close to 22.5°. In the actual shear surface, the shear zone of region 2 contains relatively few coarse particles, which have bad interlocking bond and are cut relatively smoothly. Region 2 is relatively flat

as a whole, and the ice crystal flower diagram shows that most of the angles of region 2 are close to 0°. In the actual shear surface, the first half of region 3 is relatively flat, and the second half is a relatively large depression. The ice crystal flower diagram shows that part of the angle of region 3 is close to 30°, and part of the data is close to 0°. In the actual shear surface, many small pits and protrusions are found in region 7, and most angles are close to 22.5° in the ice crystal flower diagram.

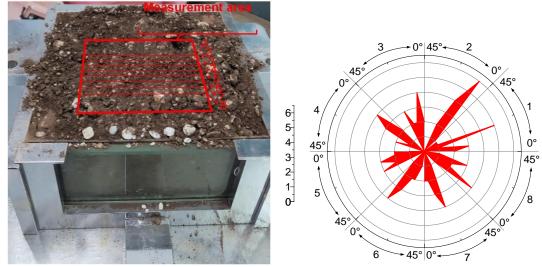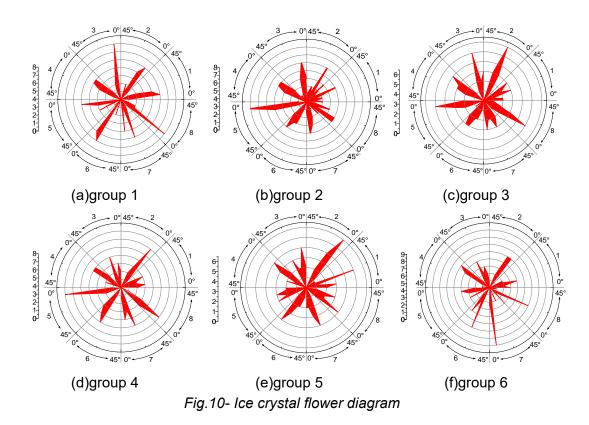*Fig.9- Comparison between actual shear surface and ice crystal flower diagram*

(a)group 1

(b)group 2

(c)group 3

(d)group 4

(e)group 5

(f)group 6

Fig.10- Ice crystal flower diagram

As can be seen from Figure 10, when the proportion of particles in this interval is low, the ice

crystal flower diagram is generally closer to 0°, which shows that the angles of two adjacent points on the shear surface are mostly small, and the shear surface is relatively flat. With the increase in the particle size in this interval, the ice crystal flower diagram gradually approaches 45°, which means that with the increase in the particles in this interval, the angle between the two points of the shear surface generally increases, the shear surface is relatively rougher, and more obviously undulated.

Effect of coarse particle content on shear surface undulation morphology

Comparison of 3D topographic map of shear surface (coarse particle content group)

The content of coarse particles in slip zone soil was studied, and the groups are divided into 40%, 50%, 60%, 70%, and 80% according to the content of coarse particles, corresponding to groups 7, 8, 9, 10, and 11, respectively. For each group, three specimens were made at 50, 100, and 150 kPa, respectively.
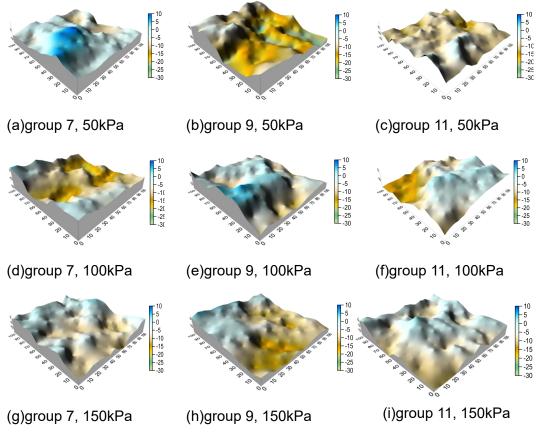

(a)group 7, 50kPa	(b)group 9, 50kPa	(c)group 11, 50kPa
(d)group 7, 100kPa	(e)group 9, 100kPa	(f)group 11, 100kPa
(g)group 7, 150kPa	(h)group 9, 150kPa	(i)group 11, 150kPa

Fig.11- Comparison of shear surface topographic map (coarse particle content, Unit: mm)

Figure 11 compares different coarse particle contents as variables and analyzes the three groups of 50, 100, and 150 kPa. Comparison at 50 kPa: The undulation of the group with 40% coarse particle content (Figure 11a) is smaller than that of the group with 60% coarse particle content (Figure 11b), and the roughness is lower. The two groups with 80% and 60% coarse particle content have more small protrusions and depressions and significantly more roughness compared with the 40%

shear failure surface. Comparison at 100 kPa: The two groups with coarse particle content of 80% and 60% (Figures 11f and 11e) are more undulating and relatively rougher. Although the shear surface of the group with coarse particle content of 40% (Figure 11d) has obvious protrusions and depressions, the undulation is smaller than that of the two groups. Comparison at 150 kPa: The shear surface morphologies of the two groups with 40% coarse particle content (Figure 11g) and 80% coarse particle content (Figure 11i) are similar, but the 80% group is rougher, and the 60% coarse particle content group (Figure 11h) has greater undulation than the 40% group. Thus, with the increase in the coarse particle content, the roughness of the shear surface of slip zone soil increases and the undulation increases. The mechanism is as follows: During the shearing process, the coarse particles in shear zone soil move and gradually rearrange along the shearing direction, forming an uneven shear surface. When the content of coarse particles is small, most coarse particles are completely wrapped by fine particles and fail to form effective contact, mainly relying on friction between particles to resist shearing. As the content of coarse particles increases, the solid matrix between coarse particles gradually forms, and the structural effect of the good interlocking bond is strong.

Statistical analysis of coordinate elevation of shear failure surface (coarse particle content group)
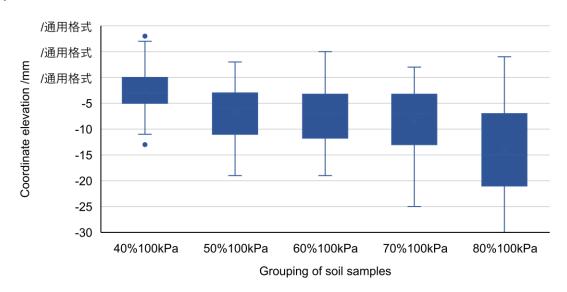

Fig.12- Elevation statistics of shear failure surface coordinate (coarse particle content group)

The shear failure surface elevation with different coarse particle contents was statistically analyzed and a box diagram was drawn. The test results under normal pressure of 100 kPa were taken as an example. The figure shows that the difference between the upper and lower edges and the difference between the upper and lower quartiles gradually increase with the increase in the coarse particle content. This finding means that the shear surface becomes relatively rough with the increase in the coarse particle content, and the undulation is more obvious. In addition, with the increase in the coarse particle content, the overall box plot of coordinate point elevation of the shear surface shows a decreasing trend.
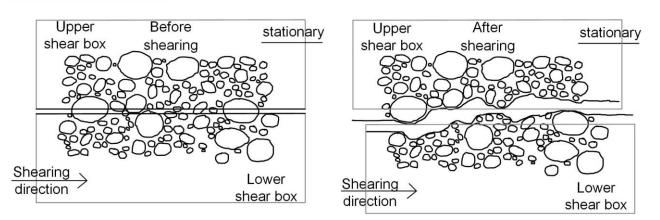
Fig.13- Schematic of the development of shear surface (group 9)

The structure in the figure (group with 60% coarse particle content) is relatively dense. The coarse particles are enough to fit well with each other and form a good solid matrix structure between them, and the fine particles are enough to fill the pores between the coarse particles, thus being a solid matrix dense structure. The protrusions in the shear zone of the structure are supported by coarse particles, which are not easily sheared off during the shear process. When the shear displacement increases continuously, the coarse particles continuously move and rotate under the action of the shear. As a result, the shear surface appears to be rougher.

Relative root mean square of undulation Z_2

According to the comparison of the calculated data (Z_2), no obvious rule exists for the particle gradation group (group 1-6), but an obvious correlation exists between the coarse particle content and the roughness of the shear surface as indicated by an analysis of the coarse particle content group. Therefore, with the coarse particle content taken as an example, quantitative analysis is conducted on the shear surface.

The roughness of the shear failure surface of slip zone soil is described by using the Z_2. A larger value corresponds to a rougher shear surface and a greater undulation. The parameter expression is as follows:

$$Z_2 = \left\{ \frac{1}{(N_x-1)(N_y-1)} \left[\frac{1}{\Delta x^2} \sum_{i=1}^{N_x-1} \sum_{j=1}^{N_y-1} \frac{\left(Z_{i+1,j+1}-Z_{i,j+1}\right)^2 + \left(Z_{i+1,j}-Z_{i,j}\right)^2}{2} + \frac{1}{\Delta y^2} \sum_{j=1}^{N_y-1} \sum_{i=1}^{N_x-1} \frac{\left(Z_{i+1,j+1}-Z_{i+1,j}\right)^2 + \left(Z_{i,j+1}-Z_{i,j}\right)^2}{2} \right] \right\}^{1/2} \quad (4)$$

In the formula, $Z_{i,j}$ are the coordinates of the "*I*"-th data point on the X-axis and the "*j*"-th data point on the Y-axis on the Z-axis, and $Z_{i+1,j+1}$ are the coordinates of the "*i+1*"th data point on the X-axis and the "*j+1*"-th data point on the Y-axis on the Z-axis. N_x and N_y represent the number of measurement data points on the x-axis and y-axis, respectively. In this test, N_x=14, N_y=14. $\triangle x$ is the spacing of measured data points along the X-axis, and $\triangle y$ is the spacing of measured data points along the Y-axis. The spacing of data points measured in both the X-axis and Y-axis is 0.8 mm, so $\triangle x = \triangle y$ =0.8mm. The 3D elevation data points of the shear surface measured in the test are

substituted into the above formula to obtain the relative root mean square of undulation Z_2 which is used to represent the roughness of the shear surface.

According to the 3D shear surface data of different soil samples, the Z_2 obtained to represent the roughness of shear surface increases with the increase in coarse grain content under each normal pressure. Through data fitting, a highly positive linear correlation existed between Z_2 and the content of coarse grains, and the correlation was high under the normal pressure of 50, 100, and 150 kPa. In addition, in the case of the same gradation, Z_2 decreases with the increase in the normal pressure, which has obvious regularity.
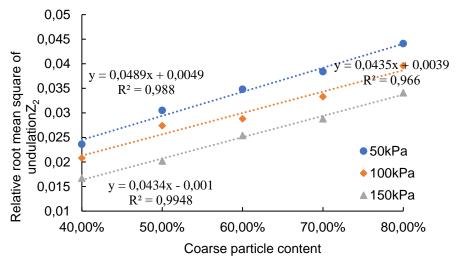

Fig.14- Relationship between shear surface roughness and coarse grain content of slip zone soil

CONCLUSION

(1)   A significant correlation exists between the undulation morphology of shear surface of the coarse-grained slip zone soil and the proportion of particles with a size between 5–20 mm. Under the same normal pressure, with the increase of particles in the interval, the shear surface undulation gradually increases, and the roughness also becomes larger. The meso-structure model shows that when the proportion of coarse particles of 5–20 mm is small, a good solid matrix cannot be formed between each particle, and the protrusion strength is not enough. Most of the protrusions are cut off during the shear process, thus resulting in low roughness.

(2)   The internal particles of well-graded soil samples have good internal structure and interlocking bond effect between coarse particles. Protrusions have high strength and are difficult to shear off. Therefore, the shear surface undulation and roughness of well-graded soil samples are more than those of poorly graded soil samples.

(3)   The increase in the normal pressure inhibits the climbing movement of soil samples along the protrusions, and the most of protrusions are sheared off. Under the same particle gradation, a great normal pressure corresponds to a smaller shear surface undulation, and with a lower roughness, the shear surface is smoother.

(4)   A highly positive linear correlation exists between Z_2 and coarse grain content. With the increase in the coarse grain content, the solid matrix between coarse particles is formed gradually, and the structural effect of the interlocking bond is strong, so the shear surface is rougher.

ACKNOWLEDGEMENTS

REFERENCES

[1]	Zhao Y. l, Zhang C. S, Wang Y. X, Lin H, 2020. Shear-related roughness classification and strength model of natural rock joint based on fuzzy comprehensive evaluation. International Journal of Rock Mechanics and Mining Sciences, Vol. 137: 104550.

[2]	Liu Q. S, Tian Y. C, Liu D. F, Jiang Y. L, 2017. Updates to JRC-JCS model for estimating the peak shear strength of rock joints based on quantified surface description. Engineering Geology, Vol. 228: 282-300.

[3]	Liu S. L, Chen S. X, Liu F, Luo H. M, Zhao W. G, 2013 Study of shear properties of weathered schist residual soil. Rock and Soil Mechanics, Vol. 34, No. 12: 3520-3526.

[4]	Cheng D. X，Xu J，Liu Z. W，Ren J. W, 2017. Experiments on Large-scale Direct Shear Strength of Coarse-grained Saline Soil. Journal of Water Resources and Architectural Engineering, Vol. 15, No. 5: 149-153.

[5]	Dong Y, Chai H. J, 2007. Experimental study on fractal character of shear surface of rock-soil aggregate mixture. Rock and Soil Mechanics, Vol. 28, No.5: 1015-1020.

[6]	Ren S. S, Zhang Y. S, Xu N. X, Wu R. J, 2021. Mesoscopic response mechanism of shear surface roughness and residual strength in gravelly sliding zone soils. Chinese Journal of Geotechnical Engineering, Vol. 43, No. 8: 1473-1482.

[7]	Singh S.K., Raval S., Banerjee B.P., 2021. Automated structural discontinuity mapping in a rock face occluded by vegetation using mobile laser scanning. Engineering Geology, Vol. 285: 106040.

[8]	Rushikesh B, Masoud Z.N, Ebrahim E, Javad S, 2021. A state-of-the-art review of automated extraction of rock mass discontinuity characteristics using three-dimensional surface models. Journal of Rock Mechanics and Geotechnical Engineering, Vol. 13, No. 4: 920-936.

[9]	Li Z.C., Liu Z.B., 2021. Influence of Particle Shape on the Macroscopic and Mesolevel Mechanical Properties of Slip Zone Soil Based on 3D Scanning and 3D DEM. Advances in Materials Science and Engineering, Vol. 2021: 9269652. DOI10.1155/2021/9269652.

[10]	Jiang J.W., Xiang. W., Zhang X.Y., 2011. Research on mechanical parameters of intact sliding zone soils of huangtupo landslide based on ct scanning and simulation tests. Chinese Journal of Rock Mechanics and Engineering, Vol. 30, No. 5: 1025-1033.

[11]	China Ministry of Housing and Urban-Rural Development. (2019),"Standard for geotechnical testing method(GB/T 50123 – 2019)" State Administration for Market Regulation, p: 344-348.

[12]	Song L. Z, Song B. W, Shen T, and Yu B, 2015. A New Numerical Simulation Method for Three-Dimensional Mesoscale Analysis of Concretes, Mathematical Problems in Engineering, Vol. 2015: 627948.

[13]	Sun Y.H., Song L.Z., Shen T., 2013. With Random Parametric Equation of Circle Inscribed Polygon Generation Algorithm and Analysis. Applied Mechanics and Materials I, Vol. 275-277: 2506-2510.